Cryogenic Liquid Sensing Using SAW Devices

B.H. Fisher[1] and D.C. Malocha[2]
School of Electrical Engineering and Computer Science
University of Central Florida, Orlando, FL. 32816-2450
brianfisher2@gmail.com[1], dcm@ece.engr.ucf.edu[2]

***Abstract*—Sensing at cryogenic temperatures is required for many critical applications, but is extremely difficult. There are a wealth of problems for cryogenic sensor devices, which include the extreme cold, which makes many sensors inoperable due to freeze-out of conduction carriers, mechanical stress and strain which impacts reliability, undesirable device heat generation in the vessel, and a host of others. In addition, consideration of sensor wiring and vessel penetration is required.**

In principle, acoustic devices can successfully operate to extremely low temperatures without any serious performance degradation. In particular, SAW devices operate as sensors, and certain embodiments are passive, wireless, and coded for multi-sensor applications. However, few results are reported on SAW devices for cryogenic applications.

Research has been performed on the use of SAW devices for operation as liquid level sensors. The initial application is for a level sensor to be used by NASA in its cryogenic liquid fuel tanks, for both ground and space vessels. The work has investigated the use of both quartz and lithium niobate devices as liquid level sensors in liquid nitrogen. In principle, the devices can operate as simple switches, with the devices turned off due to liquid SAW damping when submerged. One primary concern in using SAW devices is the survivability of the devices when shocked by rapid, large, thermal changes in the submersion and withdrawal from the liquid. Another concern is the ability of a packaged device to be reliable.

Experiments were performed on bare die, commercially available packaged devices, and on UCF fabricated devices. Samples underwent a host of rapid thermal cycling by liquid submersion and data was taken under varying test conditions. Survivability of devices and the operational parameters were measured throughout the year long study. The results found that the samples are remarkably robust. All packaged devices showed no failures in the entire study. This paper will present the experimental data and results from the study on SAW quartz and lithium niobate device operational performance parameters. A review of the various test conditions and device results will be shown. The results of this study conclude that under proper conditions, SAW devices can be used as liquid sensors at cryogenic temperatures.

I. Introduction

This paper presents the novel application of surface acoustic wave (SAW) devices to cryogenic liquid level sensing. It is documented that acoustic and shear wave devices operate well at cryogenic temperatures [1-3]. In concept SAW devices maybe ideal for cryogenic liquid level applications because the wave energy is damped by the liquid and returns to normal operation once the liquid is removed, a simple switch. Additionally, SAW devices may be coded and implemented passively and wirelessly, an added bonus. The robustness of a SAW cryogenic sensor is contingent upon the ability of the crystal substrate and metal electrodes to repeatedly withstand thermal shock resulting from large temperature gradients.

This paper addresses these concepts by first examining the behavior of commercial SAW lithium niobate ($LiNbO_3$) and quartz filters, initially hermetically sealed and then with the lids removed. Commercial devices were first examined since they would provide verification that a standard, commercial and manufacturable process could be used in the ultimate fabrication of devices for operation at cryogenic temperatures. The issue of thermal shock is investigated by the rapid temperature cycling of bare die of varying sizes, as well as packaged commercial and coded devices.

Lastly, experimentation was performed on Orthogonal Frequency Coded (OFC) devices fabricated at UCF. OFC is a passive wireless sensor technology which allows the creation of wireless sensor networks [4, 5]. An OFC sensor is composed of a uniform input transducer and two coded reflector banks, one on either side with different delays (Fig. 1). In a cryogenic liquid tank, this device serves as a switch, a temperature sensor and a unique RFID tag. This ability is ideal in a cryogenic tank environment as the level of the liquid may be quickly discerned passively and wirelessly.

II. Commercial SAW Device Performance

A. Hermetical Sealed Surface Mount Packages

Initial tests were performed on commercially available SAW parts provided by Triquint Semiconductor Inc., (formerly SAWTEK). These devices were lithium niobate ($LiNbO_3$) and quartz filters which are in surface mount packages.

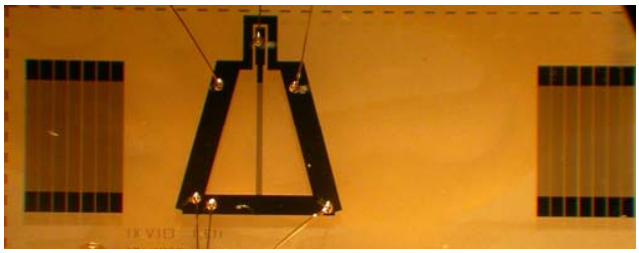

Figure 1. Dual-sided OFC SAW device on $LiNbO_3$

This work is supported by NASA KSC STTR Phase I contract # NNK06OM23C, Applied Sensor Research & Development Corp., and the McKnight Doctoral Fellowship

The following device information is provided:

Part # 523750 Quartz SAW Filter

- Die size ≈ Length: 10.5mm; Width: 2mm
- Substrate: ST Quartz, TCF: 0ppm/^{o}C (at 20^{o}C), k^2(%) ~ 0.0016, $V_{free\ surface}$ ~ 3157m/s
- Package Dimensions: 1.8cm x 0.6cm
- Center Frequency: 140MHz
- Bandwidth: 0.73MHz

Part # 856070 Lithium Niobate Filter

- Die size: ≈ Length: 10.5mm; Width: 2.5mm
- Substrate: YZ $LiNbO_3$, TCF: -94ppm/^{o}C (at 20^{o}C), k^2(%) ~ 0.046, $V_{free\ surface}$ ~ 3488m/s
- Package Dimension: 1.3cm x 0.6cm
- Center Frequency: 140MHz
- Bandwidth: 14.2MHz

One of each device was solder mounted to a printed circuit board (PCB) to which two subminiature version-A (SMA) female connectors were attached. Semi-rigid 50-ohm coaxial cables were used to connect the SMA connectors to a vector network analyzer (VNA), which extracted the RF signal. The DUT passband, S_{21}, was measured before, during and after immersion in liquid nitrogen (Figs. 2 & 3). Multiple immersions in liquid nitrogen were measured and observed to test survivability and operating changes. The measured S_{21} performance of both devices looked nearly identical after repeated temperature cycling. They exhibited lower device loss primarily due to the decrease in the aluminum thin film resistance, which is expected**.** The center frequency of the $LiNbO_3$ filter shifted upward by approximately 3MHz during immersion; the 3dB bandwidth also increased by approximately 0.14MHz. This frequency shift is to be expected based on the temperature coefficient of frequency (TCF) being positive[6]. Also evident is an increased passband ripple during submersion, this is an unexpected result. It is believed that the acoustic absorber used to damp the unwanted wave energy becomes rigid at low temperatures and no longer acts as an acoustic absorber. The quartz filter's center frequency shifted downward by approximately 0.1 MHz and the 3dB bandwidth increased by approximately 0.03MHz. The frequency shift downward is expected since the TCF is negative at low temperatures[7]. The flattened passband at low temperature is also consistent with a time echo due to the loss of acoustic damping at the crystal edges.

Equally as important as the device performance over repeated cycles was that of the test fixture; the solder, PCB and SMA connectors all survived without any evident electrical or mechanical damage. This allowed the design of a test fixture that could facilitate quick measurement of a large number of samples without soldering. It is necessary to cycle large number of devices in order to verify the previously observed behavior.

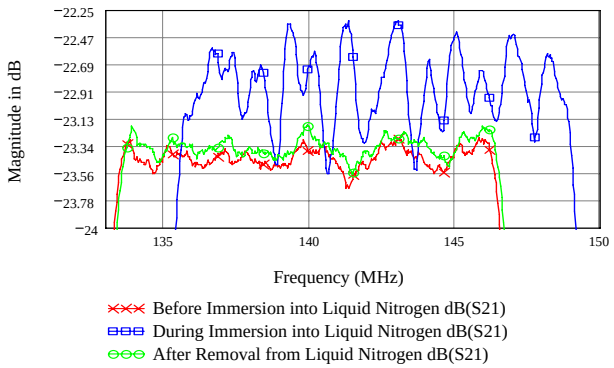

Figure 2. Hermetically sealed lithium niobate filter passband comparisons, before during and after submersion in liquid nitrogen

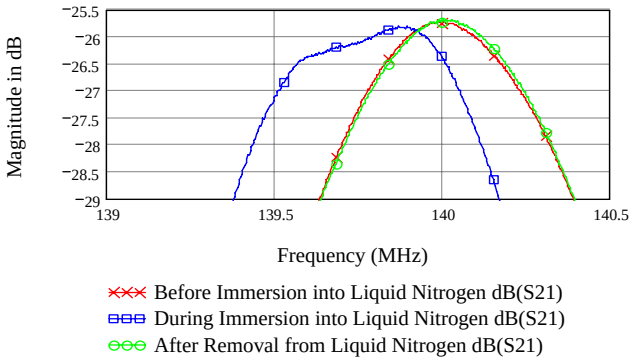

Figure 3. Hermetically sealed quartz filter passband comparisons, before during and after submersion in liquid nitrogen

This fixture consisted of a PCB to which two SMA female connectors were soldered; a powerful clip was used to enforce a firm contact between the devices and the PCB. Ten samples of each filter were temperature cycled twenty times and measured before the first cycle and after the last. A comparison of the first and last cycle confirmed the previous observation: there is no degradation in the passband response as a result repeated of thermal cycling.

B. Opened Lid Surface Mount Devices

This phase of experiments focused on examining the device behavior after the die has direct contact with cryogenic liquid. To accomplish this, a variety of apertures were cut in the lids of the hermetically sealed packages. Initially three 0.454mm holes were drilled in each of the cases. One hole was drilled at either end of the case and one in the middle. Using this method of hole placement in combination with lowering the chip length-wise into liquid nitrogen allows air to escape the case's cavity thereby allowing cryogenic fluid to flow over the substrate. Once the liquid is in contact with the crystal surface, the SAW couples into the liquid and 40-50 dB of attenuation occurs which is its "off state," once removed it returned to its peak. The wave energy became damped as the die warmed and humidity condensed. After approximately 35 minutes normal operation was restored. Larger apertures were placed in the lids in order to study device operation. The devices were tested with 1mm x 6mm slits at either end of the

package (Fig. 4). These slit lid devices were cycled from room to cryogenic temperature six times, a plot of the passband after each cycle is shown in figures 5 and 6. The random attenuation of the passband with each successive cycle indicates that particulates and contamination are increasingly growing on the active area of the die after the condensation evaporates. The randomization here is possibly due to particulates of metal on the transducers, as a result of drilling and cutting the package lid. These issues would not occur in practice since contamination due to lid removal would not occur and condensation will also be eliminated in a cryogenic tank environment. The important result from this phase of testing is that the devices never ceased working, an indication that thermal shock is not an issue under these testing conditions.

Figure 4. $LiNbO_3$ packaged device soldered to PCB with 1mm x 6mm silts in both ends of the package

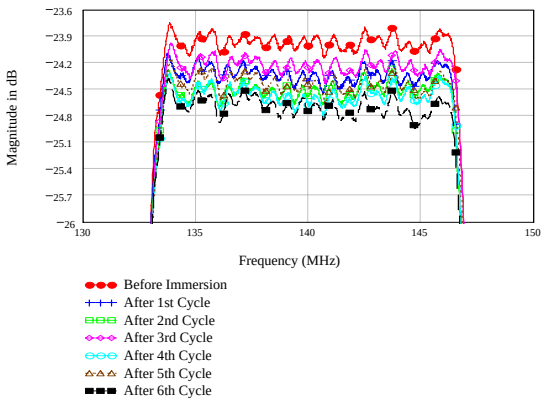

Figure 5. Passband response of repeated cycling of $LiNbO_3$ device with 1mm x 6mm slits in the package lid.

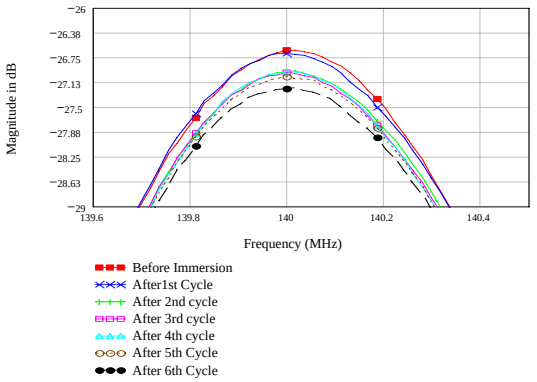

Figure 6. Passband response of repeated cycling of quartz device with 1mm x 6mm slits in the package lid.

C. Cryogenic Head Space Temperature Cycling

To simulate the environment of a cryogenic tank; a glass dewar environment was modified such that the liquid nitrogen was contained, and a lid with feedthroughs allowed the devices under test to be lowered and raised in the flask. The lid kept the gas volume in the head space at a near cryogenic temperature, similar to what is expected in a real tank. The head space is much cooler than room temperature and is in a water free environment which will prevent condensation of the devices. The lid for the test flask was constructed using Styrofoam. This material was chosen for its good insulation properties and ease of handling. Two semi-rigid transmission lines pierced this lid in order to connect the device under test to the VNA. The lid was sealed for minimal openings left by the transmission lines piercing the lid. In addition to measuring the passband with the VNA, the real time behavior of the passband was captured using digital video. The time-code from digital video is very accurate and serves as an excellent means of extracting the switching speeds of the filters. The turn-off switching cycle was designated as the time from submersion until the passband was obscured in noise; and the turn-on cycle was designated as the time from removal from cryogenic fluid until the passband returned to normal, or near normal, room temperature operation. The human error in these times is approximately ±0.2s. The testing fixture was the same as previously reported—a PCB with SMA connectors and the surface mount SAW filters which were all solder mounted. The devices were oriented vertically with respect to the surface of the cryogenic fluid so that the cryogenic liquid will invade through the lower slits and force air out of the cavity during the submersion process, and the converse process occurs during removal. The cycling procedure as before was: measure S_{21} response of device prior to submersion, submerge in cryogenic fluid for a period of time, then measure S_{21} response once the device is removed.

1) Temperature Head Space Cycling of Devices with Slit lids

Devices were immersed in the liquid nitrogen and the resulting S_{21} response was observed on the VNA. The lithium niobate devices turned-off in 0.32 seconds on average and the quartz turned-off in 0.55 seconds on average. It was hypothesized that the turn off times are not instantaneous because liquid nitrogen boils and evaporates when it makes initial contact with the room temperature chip surface, forming a vapor barrier until equilibrium is reached. The turn-on times however, were fairly long because it is most likely a function of the actual device temperature, the area of the slits, and the liquid adhesion properties on the active die surface. The lithium niobate devices turned-on in 40.1 seconds (average) and the quartz turned-on in 20 seconds (average) after removal from the liquid. The difference in turn-on times is most likely due to the size of the device packages, the topology of the active device areas and the difference in the package slit openings. The quartz is a simple in-line SAW filter with an unapodized input transducer and an

apodized output transducer. The fractional bandwidth is small and the impulse response longer than that of the $LiNbO_3$ filter. The niobate device however, has both apodized input and output transducers with a multi-strip coupler between the transducers and damping material between the transducer and the couplers (Figs. 7 & 8). The active area of the two filters are dramatically different, as well as topography and acoustic absorber areas. The S_{21} responses produced a practically constant passband response, with only a few tenths of a dB in amplitude variation, after repeated cycling for both quartz and lithium niobate (Figs. 9 & 10).

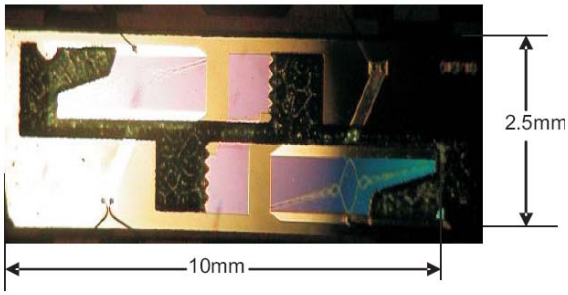

Figure 7. Photo of $LiNbO_3$ device topology

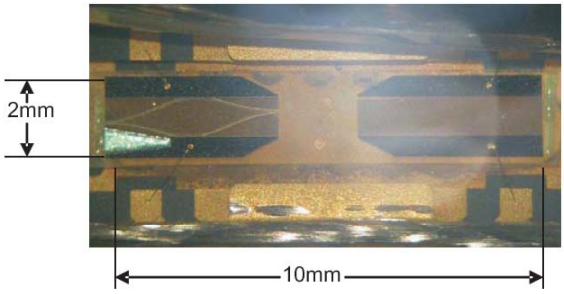

Figure 8. Photo of quartz device topology

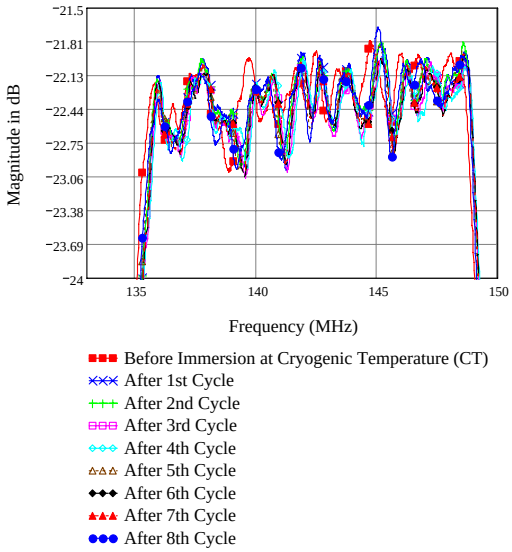

Figure 9. $LiNbO_3$ cryogenic head-space temperature cycling, after lid removal.

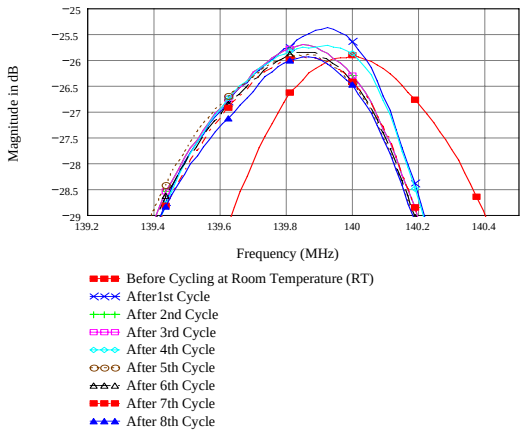

Figure 10. Quartz cryogenic head-space temperature cycling, after lid removal.

2) Package Lid Removal and Inspection

The package lids were removed with the use of a Dremel tool and grinding wheel. In order to prevent the lid from falling onto the delicate die, only three sides of the package was opened then the lid was bent and broken off. Upon inspection with a microscope, the transducers were littered with microscopic pieces of metal on the die surface and throughout the package cavity due to the lid removal process. Cleaning failed to remove many of these pieces of metal but the devices still worked well and it is was determined that the experiments could move forward.

3) Temperature Head Space Cycling of Opened Devices

The testing of the devices without the lid proceeded the same as with the slit experiments as previously discussed. The lithium niobate devices turned-off in 0.33 seconds on average and the quartz devices turned-off in 0.59 seconds on average, very similar to results of the slit-open devices. The lithium niobate devices turned-on in 6.38 seconds on average and the quartz devices turned-on in 4.22 seconds on average. The device turn-on times were much faster than reported in the previous section, most likely due to the difference in the opening area. The difference in turn-on time between the quartz and niobate devices is most like due to the size of the device die and packages. The S_{21} responses revealed a near constant passband after repeated cycling for lithium niobate. The S_{21} response of the quartz device, however, showed a gradual increase in insertion loss with each successive cycle. Once the device was removed from the test fixture, allowed to return to room temperature and measured, the insertion loss returned to a value closer to the value before the temperature cycling began. A second cycle revealed a similar result, and a second device was tested with similar outcome. However, depending on the device and the immersion cycle, the insertion loss would show tendencies of both increasing and decreasing slightly. It is possible that the contamination of the die surface due to the Dremel tool lid removal is having an effect on the performance of the quartz devices. Interestingly, similar contamination is present on the niobate device yet their performance is as expected. The device designs on the quartz

and niobate are very different due to their difference in bandwidth. The die of both devices were inspected with a microscope and in both cases the cryogenic liquid cycling had actually reduced the quantity of the metal pieces on the die area. Another possible culprit of the slow degradation of the quartz passband may be micro-cracks in the substrate. There is currently no evidence to confirm or deny this speculation. The quartz loss issue will be addressed in the thermal shock of experiments.

4) Parallel Oriented Devices

This experiment is intended to discover if the device's orientation when lowered into liquid nitrogen has an effect on its operation. The test fixture was redesigned to orient the longer length of the die parallel to the surface of the liquid nitrogen; this means that the transducer's fingers are normal to the liquid. The devices response was measured using the technique as previously discussed.

When compared to previous measurements with a 90^o rotation compared to the current test device orientations, the turn-off times were approximately the same as with prior experiments, when the margin of error is considered. The quartz device's turn-on times were slightly longer than before (approximately a half a second on average). The lithium niobate devices, however, showed a 3.6 fold increase in turn-on time. It is conjectured that the primary method for device turn-on is the removal of liquid from the transducers by means of gravity; therefore, the switching speeds for both devices should be approximately the same. However, there are large differences in the device layout topography and it is presumed that switching speed differences are mainly due to the physical layout of the devices (as previously discussed).

III. Thermal Shock

Quartz and $LiNbO_3$ die are vulnerable to fracture attributable to thermal shock due to: poor thermal conductivity, large temperature change (~213^oC) and the dicing process. Quartz and lithium niobate wafers were diced by both Vectron Int. and UCF. The die from Vectron were larger (~ 12mm x 18mm x 0.5mm) than the die diced from UCF (~ 9.5mm x 4.5mm x 0.36mm). This was done purposefully to see if the effect of size in the shock tests. Tests would investigate the relative effects between die size, dicing method and thermal shock. It should be remembered that none of the packaged devices failed during the numerous temperature cycling. The die edges were inspected using a metallurgical microscope on various magnifications and a polarizing lens prior to any submersion into the liquid nitrogen. The die edges are stressed and chipped during normal dicing operations; consequently, cracks from thermal stress are likely to propagate from these areas. Based on our inspection and qualitative analysis, both the Vectron and UCF samples had very similar edges after dicing. The dies were temperature cycled from room to cryogenic temperature and then inspected again. Five lithium niobate die (larger samples) were cycled, four fractured violently upon submersion into the liquid nitrogen. All the smaller samples survived. Upon inspection with a microscope, it was not clear exactly where the cracks in the lithium niobate originated. The sample that survived looked just as it did before cycling, i.e. no excessive cracks or chipping (other than the edges) were evident. All the quartz samples survived and after microscopic inspection appeared unchanged by the temperature cycling. In order to perform automated die cycling, a temperature cycling apparatus was constructed; this machine kept the die in the head space for ten minutes then submerged the die for ten minutes. The temperature difference was from the cryogenic dewar head space temperature to the liquid nitrogen submersion (~104^oC). Two samples each of lithium niobate and quartz from UCF and Vectron were examined by microscope then cycled for fours hours, using the temperature cycling machine. None of the die broke or showed any cracking or fracture from the cycling process.

The results of these tests confirm what was expected. First, quartz is known to be a fairly robust material, is weakly piezoelectric, non-pyroelectric to any degree, and has a relatively small expansion coefficient. Manufacturing SAW quartz devices over the past 30 years has been fairly easy and thermal shock has typically been no problem. On the other hand, lithium niobate has higher piezoelectric constants than quartz, is pyroelectric, and has larger expansion coefficients than quartz. Manufacturing SAW niobate devices over the past 30 years has resulted in more controlled manufacturing processes than quartz, especially in regards to thermal shock.

IV. OFC Device Performance

The last phase of experimentation involved an examination of OFC devices in response to temperature cycling. UCF fabricated OFC device using a common method: contact lithography, ebeam metallization and lift-off. The devices were fabricated on $LiNbO_3$, the die sizes were (~14mm x 4mm x 0.36mm). This is a one port device and reflections are easily visible in the time domain, thus, the S_{11} time domain response was examined and recorded in order to asses device behavior and switching speed. The device was head space cycled in order to determine its switching speeds. It turned-off in an average time of 0.6seconds and turned-on in an average of 3.7seconds. Since the OFC device uses reflectors the signal has to traverse the die surface twice, thus the signal loss is more sensitive to surface damage than the commercial filters and yet there was no degradation of the passband as compared to the commercial filters (Fig. 11). This suggests that the previous behavior was in fact due to metal remnants from cutting the package lid. A close-up of the second reflector bank shows the delay of the reflection decreased when submerged in liquid nitrogen (Fig. 11); the first reflector bank exhibited an equivalent response. This makes sense since the material TCF of $LiNbO_3$ is positive, and TCD is negative. The OFC device was also cycled from room to cryogenic temperature five times in order to asses its response to thermal shock. A comparison of the first and last cycled

revealed no serious degradation (Fig. 12). The aluminum electrodes were inspected before and after cycling to determine if they were damaged by the cycling process, they looked practically the same, cleaner in some cases. A performance summary of the OFC and commercial devices is presented in Table 1.

V. Conclusion

The most enlightening aspect of the temperature cycling tests is the fact that by mounting the devices into a commercial package using standard mounting techniques, the thermal shock at cryogenic temperatures seems to be controllable. Hundreds of cycles of commercial devices at cryogenic liquid to gas, or even room temperature, have resulted in no device failures. This is a clear indication that producing a SAW liquid sensor that operates at cryogenic temperatures is feasible on either quartz or lithium niobate.

$LiNbO_3$	**Off (sec)**	**On (sec)**	**Quartz**	**Off (sec)**	**On (sec)**
Slits	0.3	40.4	Slits	0.6	20.0
Filter with Open Lid (Vertical Orientation)	0.3	6.4	Filter with Open Lid (Vertical Orientation)	0.6	4.2
Filter with Open Lid (Horizontal Orientation)	0.4	23.0	Filter with Open Lid (Horizontal Orientation)	0.6	5.2
OFC Device (Vertical Orientation)	0.6	3.7			

Table 1. Performance summary; Off-submersion until the device's signal is lost in noise; On-time after removal from liquid for device to recover to its nominal insertion loss in dry air.

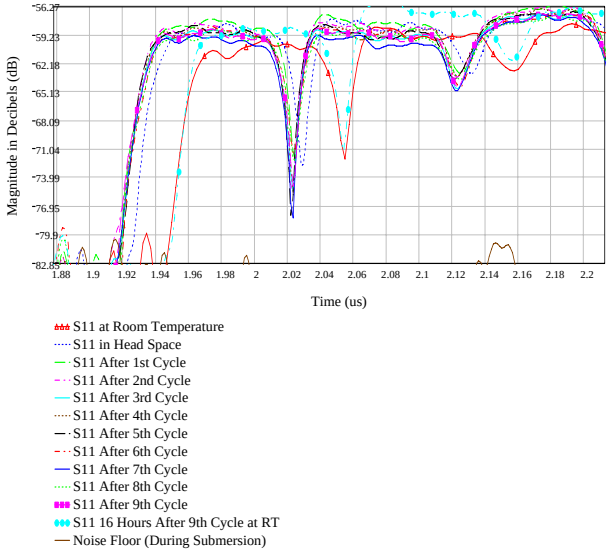

Figure 11. Close-up of second reflector bank of OFC device. This shows the response to repeated temperature cycling from headspace to liquid. The first reflector bank exhibited an equivalent response.

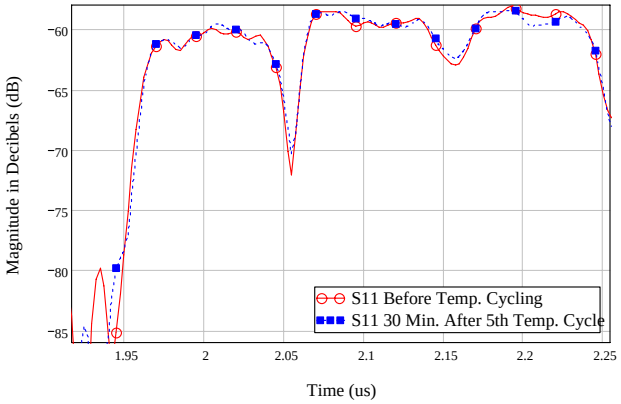

Figure 12. Close-up of the response of the second reflector bank of OFC device after five temperature cycles from room to cryogenic temperature. The first reflector bank exhibited an equivalent response.

Acknowledgment

The authors would like to thank Triquint Semiconductor Inc. for furnishing commercial SAW filters and Vectron Intl. for furnishing die samples. The authors are grateful to Dr. Robert Youngquist, NASA-KSC for his continuing support discussions and suggestions. The authors are grateful for the NASA STTR Phase I funding, to Applied Sensor Research & Development Corp. and the McKnight Doctoral Fellowship.

References

[1] B. R. McAvoy and H. L. Salvo, Jr., "Cryogenic Experiments with Microwave Acoustic Resonators," *IEEE Ultrasonics Symposium*, pp. 343-348, 1986.

[2] K. Yamanouchi, H. Nakagawa, and H. Odagawa, "GHz-range surface acoustic wave low loss filter at super low temperature," *Joint Meeting of the European Frequency and Time Forum and the IEEE International Frequency Control Symposium*, vol. 2, pp. 911-914 vol.2, 1999.

[3] Y. Aoki, Y. Wada, Y. Sekimoto, W. Yamaguchi, A. Ogino, M. Saitoh, R. Nomura, and Y. Okuda, "Application of Surface Acoustic Wave Sensors for Liquid Helium-4 and Helium-3," *Journal of Low Temperature Physics*, vol. 134, pp. 945-958, 2004

[4] D. C. Malocha, D. Puccio, and D. Gallagher, "Orthogonal frequency coding for SAW device applications," *IEEE Ultrasonics Symposium*, vol. 2, pp. 1082-1085, 2004.

[5] D. Puccio, D. C. Malocha, and N. Saldanha, "Multiple access SAW sensors using orthogonal frequency coding," *IEEE Sensors*, pp. 723-726, 2005.

[6] J. Hornsteiner, E. Born, G. Fischerauer, and E. Riha, "Surface acoustic wave sensors for high-temperature applications," *IEEE International Frequency Control Symposium*, pp. 615-620, 1998.

[7] T. E. Parker and G. K. Montress, "Precision surface-acoustic-wave (SAW) oscillators," *IEEE Transactions on Ultrasonics, Ferroelectrics and Frequency Control*, vol. 35, pp. 342-364, 1988.